

## Magneto-Stimulated Hydrodynamic Control of Electrocatalytic and Bioelectrocatalytic Processes

Eugenii Katz and Itamar Willner\*

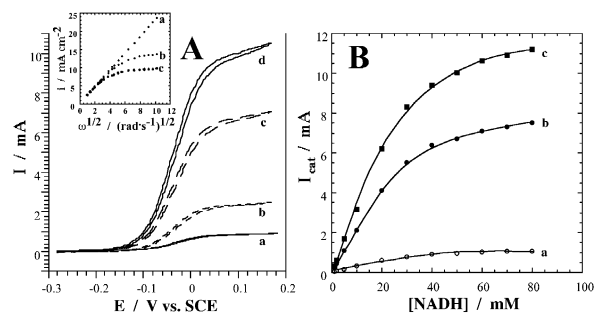
*Institute of Chemistry, The Hebrew University of Jerusalem, Jerusalem 91904, Israel*

Received April 4, 2002

Recent efforts are directed to the magnetic-field switching of electrocatalytic and bioelectrocatalytic processes.<sup>1</sup> Several applications of magneto-controlled electron-transfer reactions, such as selective dual biosensing and stimulated electrogenerated chemiluminescence were suggested.<sup>2</sup> Magnetic particles functionalized with chemical or biological components are extensively used as a "collection tool" for the concentration and the localization of chemical or biochemical components.<sup>3</sup> Different applications of chemically modified magnetic particles were reported, including transport and concentration of enzymes,<sup>4</sup> DNA,<sup>5</sup> or cells.<sup>6</sup> Here we wish to report on the concentration of redox-functionalized magnetic particles on an electrode using an external magnet mounted on a rotating motor. The rotation of the external magnet results in rotation of the redox-functionalized magnetic particles on the electrode support. That is, the magnetic particles behave as microelectrodes with circular rotation, and the electrocatalytic and bioelectrocatalytic transformations at the particles' interface are controlled by the hydrodynamics rather than by diffusion. This leads to amplified electro- and bioelectrocatalyzed processes as a result of enhanced mass transport to the electrode. Besides the fundamental interest in such systems, the method represents a novel amplification concept in bioelectronics.

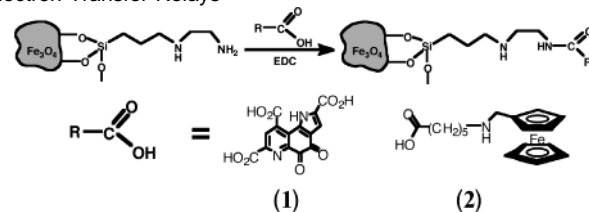
Magnetic particles ( $\text{Fe}_3\text{O}_4$ , ca. 1  $\mu\text{m}$  average diameter, saturated magnetization ca. 65  $\text{emu}\cdot\text{g}^{-1}$ ) were prepared according to the published procedure<sup>7</sup> without including the surfactant into the reaction medium. The magnetic particles were silanized with [3-(2-aminoethyl)aminopropyl]trimethoxysilane and then functionalized with pyrroloquinoline quinone, PQQ (1), or with *N*-(ferrocenylmethyl)aminohexanoic acid (2), using 1-ethyl-3-(3-dimethylaminopropyl)-carbodiimide, EDC, as a coupling reagent, Scheme 1. The PQQ-functionalized magnetic particles attracted to a bottom Au electrode (0.24  $\text{cm}^2$ ) by the external permanent magnet (NdFeB/Zn-coated magnet, 18 mm diameter, providing 0.2 kOe at the electrode surface), reveal a reversible cyclic voltammogram,  $E^\circ = -0.13$  V (vs SCE), pH = 7.0, indicating an average surface coverage of  $7.5 \times 10^3$  PQQ units per particle. The cyclic voltammogram of the PQQ units associated with the magnetic particles is independent of the rotation speed of the external magnet, indicating that the redox units are confined to the electrode. The PQQ-functionalized magnetic particles act as an electrocatalyst for the oxidation of 1,4-dihydronicotinamide adenine dinucleotide, NADH, in the presence of  $\text{Ca}^{2+}$  ions.

Figure 1A shows the cyclic voltammograms observed upon the PQQ-magnetite-mediated electrocatalyzed oxidation of NADH, 50 mM, at different rotation speeds of the external magnet. Figure 1B shows the calibration curves corresponding to the anodic currents originating in the presence of different concentrations of NADH at variable rotation speeds of the external magnet. From Figure



**Figure 1.** (A) Cyclic voltammograms of a Au-electrode with the magnetically attracted PQQ-functionalized magnetic particles (10 mg) in the presence of 50 mM NADH upon rotation of the magnet (rpm): (a) 0, (b) 10, (c) 100, (d) 1000. Potential scan rate, 5  $\text{mV}\cdot\text{s}^{-1}$ . Inset: Levich plot of the electrocatalytic oxidation of NADH, 50 mM, at  $E = 0.1$  V: (a) Theoretical plot according to eq 1 for the PQQ-functionalized RDE, (b) Experimental plot for the PQQ-functionalized RDE, (c) Experimental plot for the PQQ-functionalized magnetic particles. (B) Calibration plots for the amperometric detection of NADH ( $E = 0.1$  V) upon rotation of the magnet (rpm): (a) 0, (b) 100, (c) 1000. The data were recorded in 0.1 M Tris-buffer, pH 7.0 with 20 mM  $\text{CaCl}_2$ .

### Scheme 1. Functionalization of the Magnetic Particles with the Electron Transfer Relays



1A and B it is evident that the resulting electrocatalytic currents increase as the rotation speed of the external magnet is elevated (the theoretical relation  $I_{\text{cat}} \propto \omega^{1/2}$  is observed at low rotation speeds). In a control experiment, PQQ-functionalized silica particles that gravimetrically settle on the Au-electrode were subjected to different rotation speeds of the external magnet in the presence of NADH. No effect of the external rotating magnet on the resulting electrocatalytic current was observed. This implies that the circular rotation of the magnetic particles on the electrode support leads to the increased electrocatalytic anodic currents upon rotation of the external magnet due to hydrodynamic control of the substrate mass transport to the electrode.

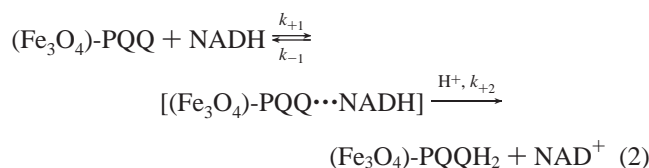
Rotating disk electrodes were extensively applied for the characterization of bioelectrocatalytic transformations.<sup>8</sup> The effect of rotation speed on the electrocatalyzed oxidation of NADH by the PQQ-magnetic particles was quantitatively analyzed by the Levich relation, and the interfacial electron-transfer kinetics was further characterized by the Koutecky–Levich treatment. A Au-rotating disk electrode (RDE) functionalized with a PQQ monolayer ( $2.1 \times 10^{-10}$   $\text{mol}\cdot\text{cm}^{-2}$ ) attached to the electrode surface via a

\* To whom correspondence should be addressed. E-mail: willnea@vms.huji.ac.il.

cystamine monolayer<sup>9</sup> was used to compare it with the PQQ-functionalized magnetic particles. Curves (a) and (b), Figure 1A, inset, show the theoretically calculated current densities using the Levich equation,<sup>10</sup> eq 1, (where  $D_{\text{NADH}} = 2.4 \times 10^{-6} \text{ cm}^2 \cdot \text{s}^{-1}$  is the NADH diffusion coefficient,<sup>11</sup> and  $\nu = 0.01 \text{ cm}^2 \cdot \text{s}^{-1}$  is the kinematic viscosity of water) and the experimental electrocatalytic current densities,  $i_{\text{cat}}$ , of the Au-RDE in the presence of NADH, 50 mM, as a function of rotation speed ( $\omega^{1/2} \text{ rad} \cdot \text{s}^{-1}$ ), respectively. Figure 1A inset, curve (c), shows the experimental  $i_{\text{cat}}$  of the PQQ-functionalized magnetic particles in the presence of NADH, 50 mM. Note that the amount of the immobilized PQQ on the Au-RDE and on the magnetic particles (10 mg) was the same and that the currents observed for the PQQ-magnetic particles depicted in Figure 1A inset, curve (c), are normalized in respect to the current of the PQQ-functionalized Au-RDE, at low rotation speeds. This allows extracting the effective surface area of the magnetic particles and the effective surface coverage of PQQ on the magnetic particles ( $4.7 \times 10^{-11} \text{ mol} \cdot \text{cm}^{-2}$ ).

$$i_{\text{cat}} = 0.62 \cdot n \cdot F \cdot D_{\text{NADH}}^{2/3} \cdot \nu^{-1/6} \cdot [\text{NADH}] \cdot \omega^{1/2} \quad (1)$$

Replotting the curves (b) and (c) shown in Figure 1A, inset, in the form of the Koutecky–Levich plot (see the Supporting Information) enabled us to determine the overall electrochemical rate constants,  $k_{\text{overall}}$ , for the oxidation of NADH by the PQQ-functionalized particles and by the PQQ-modified RDE,  $5.5 \times 10^4$  and  $4.5 \times 10^4 \text{ M}^{-1} \cdot \text{s}^{-1}$ , respectively. Following the scheme suggested by Gorton<sup>12</sup> for the electrocatalyzed oxidation of NADH, eq 2,  $k_{\text{overall}}$  is given by eq 3. By the determination of the  $k_{\text{overall}}$  values for the PQQ-functionalized magnetic particles in the presence of different concentrations of NADH (data given in the Supporting Information), we find that  $k_{+2} = 20 \text{ s}^{-1}$  and  $K_{\text{M}} = 0.6 \text{ mM}$ . These values are very similar to those derived for the electrocatalyzed oxidation of NADH by a PQQ-monolayer associated with the RDE.



$$(k_{\text{overall}})^{-1} = K_{\text{M}}/k_{+2} + [\text{NADH}]/k_{+2} \quad (3)$$

where

$$K_{\text{M}} = (k_{-1} + k_{+2})/k_{+1}$$

The magnetic-field stimulated enhancement of the electrocatalytic currents generated by the circular rotation of redox-functionalized magnetic particles was also demonstrated for bioelectrocatalytic transformations. The magnetic particles functionalized with the ferrocene derivative **2** were attracted to the Au-electrode and rotated on the conducting support by means of the external rotating magnet. The quasi-reversible redox-wave of the ferrocene units,  $E^\circ = 0.32 \text{ V}$ , is independent of the rotation of the external magnet. Figure 2A shows the cyclic voltammograms of the ferrocene-functionalized magnetic particles in the presence of glucose oxidase (GOx),  $1 \times 10^{-5} \text{ M}$ , and glucose, 50 mM, at different rotation rates of the external magnet. Figure 2B shows the calibration curves corresponding to the amperometric responses of the system at different concentrations of glucose and variable speeds of rotation of the external magnet. The electrocatalytic anodic currents increase as the external rotation speed of the magnet is elevated. Control

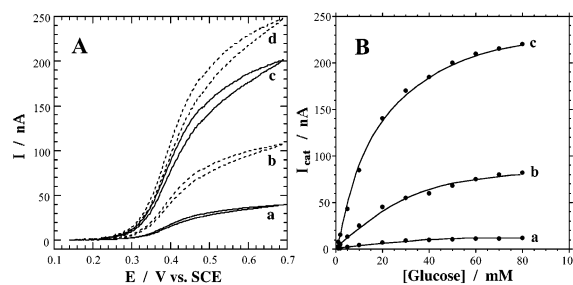


**Figure 2.** (A) Cyclic voltammograms of a Au-electrode with the magnetically attracted (**2**)-functionalized magnetic particles (6 mg) in the presence of GOx,  $1 \times 10^{-5} \text{ M}$ , and glucose, 50 mM upon rotation of the magnet (rpm): (a) 0, (b) 10, (c) 100, (d) 400. Potential scan rate,  $5 \text{ mV} \cdot \text{s}^{-1}$ . (B) Calibration plots for the amperometric detection of glucose ( $E = 0.5 \text{ V}$ ) upon rotation of the magnet (rpm): (a) 0, (b) 100, (c) 400. The data were recorded in 0.1 M phosphate buffer, pH 7.0.

experiments reveal that the electrocatalytic anodic currents are observed only in the presence of glucose oxidase and glucose, and that no effect of the rotation speed of the external magnet on the electrocatalytic anodic currents generated by ferrocene-functionalized  $\text{SiO}_2$  particles is observed.

To summarize, we demonstrate the novel application of redox-functionalized magnetic particles and an external magnetic rotor as a coupled system for enhancing electrocatalytic and bioelectrocatalytic processes. The rotating magnetic particles enhance the mass transport of substrates to the electrode and hence enhance the electrochemical transformations at the conducting support. The coupling of the enhanced currents, observed upon the rotation of electrocatalytically active magnetic particles, with biomaterial recognition events at the particles represents a novel amplification means in biosensors and bioelectronic devices.

**Acknowledgment.** This research is supported by the German-Israel Program (DIP).

**Supporting Information Available:** Koutecky–Levich plots corresponding to the experimental data (b) and (c) shown in Figure 1, inset (PDF). This material is available free of charge via the Internet at <http://pubs.acs.org>.

## References

- (1) (a) Hirsch, R.; Katz, E.; Willner, I. *J. Am. Chem. Soc.* **2000**, *122*, 12053–12054.
- (2) (a) Katz, E.; Sheeney-Haj-Ichia, L.; Bückmann, A. F.; Willner, I. *Angew. Chem., Int. Ed.* **2002**, *41*, 1343–1346. (b) Sheeney-Haj-Ichia, L.; Katz, E.; Wasserman, J.; Willner, I. *Chem. Commun.* **2002**, 158–159.
- (3) (a) Dickson, D. P. E.; Walton, S. A.; Mann, S.; Wong, K. *NanoStruct. Mater.* **1997**, *9*, 595–598. (b) de Cuyper, M.; Joniau, M. *Biotechnol. Appl. Biochem.* **1992**, *16*, 201–210. (c) Carpenter, E. E. *J. Magnetism Magnetic Mater.* **2001**, *225*, 17–20. (d) Matsunaga, T.; Takeyama, H. *Supramol. Sci.* **1998**, *5*, 391–394.
- (4) Liao, M.-H.; Chen, D.-H. *Biotechnol. Lett.* **2001**, *23*, 1723–1727.
- (5) (a) Wang, J.; Xu, D.; Polsky, R. *J. Am. Chem. Soc.* **2002**, *124*, 4208–4209. (b) Wang, J.; Kawde, A.-N. *Electrochem. Commun.* **2002**, *4*, 349–352.
- (6) Sonti, S. V.; Bose, A. *J. Colloid Interface Sci.* **1995**, *170*, 575–585.
- (7) Shen, L.; Laibinis, P. E.; Hatton, T. A. *Langmuir* **1999**, *15*, 447–453.
- (8) Razumas, V.; Jasaitis, J.; Kulys, J. *Bioelectrochem. Bioenerg.* **1983**, *10*, 427–439.
- (9) Katz, E.; Lötzbeyer, T.; Schlereth, D. D.; Schuhmann, W.; Schmidt, H.-L. *J. Electroanal. Chem.* **1994**, *373*, 189–200.
- (10) Bard, A. J.; Faulkner, L. R. *Electrochemical Methods: Fundamentals and Applications*, Wiley: New York, 1980.
- (11) Moiroux, J.; Elving, P. J. *J. Am. Chem. Soc.* **1980**, *102*, 6533–6538.
- (12) Gorton, L. *J. Chem. Soc., Faraday Trans. 1* **1986**, *82*, 1245–1258.

JA0264145